

471 **A Appendix**

472 **A.1 Active Learning Acquisition Functions**

473 Traditional BO acquisition functions, such as EI and LCB, use the computed means and variances  
 474 from a surrogate model to compute an acquisition value; maximizing this acquisition value guides  
 475 sampling of the manifold [7, 32, 12]. However, these traditional acquisition functions are static,  
 476 such that they do not actively use any information about the performance of previously sampled  
 477 experiments to guide sampling. Hence, we implement an active learning approach into the acquisition  
 478 functions to develop two novel functions, EI Abrupt and LCB Adaptive, that dynamically adapt  
 479 their sampling based on the quantity and quality of previously sampled experiments. In contrast to a  
 480 static acquisition function, these dynamic acquisition functions are initialized with an initial set of  
 481 hyperparameter values to guide their search but then tune these values as sampling progresses. The  
 482 developed EI Abrupt and LCB Adaptive functions are used within the ZoMBI framework to further  
 483 accelerate optimization and avoid pigeonholing, see line 9 of Algorithm 1.

484 **EI Abrupt** uses actively learned information about the quality of previously measured experiment  
 485 target values,  $y$ , to change sampling policies. For example, if the value of  $y$  plateaus for three or  
 486 more experiments in a row, EI Abrupt will abruptly switch from a greedy sampling policy to a  
 487 more explorative sampling policy. Specifically, this information feedback received by the function  
 488 determines if the current round of sampling should exploit the surrogate mean values,  $\mu(X)$ , or  
 489 explore the surrogate variances,  $\sigma(X)$ . EI Abrupt computes an acquisition value,  $a \in [0, 1]$ , for  
 490 a given  $X$ , wherein the  $X$  with the highest  $a$  is selected by the acquisition function as the next  
 491 suggested experiment to measure. EI Abrupt is implement for a minimization problems as:

$$a_{\text{EI Abrupt}}(X, y; \beta, \xi, \eta) = \begin{cases} (\mu(X) - y^* - \xi) \Phi(Z) + \sigma(X)\psi(Z), & \text{if } |\nabla\{y_{n-3\dots n}\}| \leq \eta \\ \mu(X) - \beta\sigma(X), & \text{otherwise} \end{cases} \quad (3)$$

$$Z = \frac{\mu(X) - y^* - \xi}{\sigma(X)},$$

492 where  $y^*$  is the lowest measured target value thus far (*i.e.*, the running minimum),  $\Phi(\cdot)$  is the  
 493 cumulative density function of the normal distribution,  $\psi(\cdot)$  is the probability density function of  
 494 the normal distribution, and  $|\nabla\{y_{n-3\dots n}\}|$  is the absolute value of the gradient of the set of target  
 495 values of the last three sampled experiments; a gradient of 0 indicates a plateau. Moreover,  $\beta = 0.1$ ,  
 496  $\xi = 0.1$ , and  $\eta = 0$  are hand-tuned initialization hyperparameters used for the rest of the paper for  
 497 EI Abrupt. These hyperparameters were selected based on *a priori* domain knowledge of EI Abrupt  
 498 performance on a variety of different problems. The most important hyperparameter for efficient  
 499 sampling is  $\beta$ , whose ideal value is non-obvious, but it is found that  $\beta = 0.1$  allows EI Abrupt to  
 500 switch into an explorative sampling policy while still having a strong weight on the surrogate means,  
 501 implying that exploration does not veer far.

502 **LCB Adaptive** uses actively learned information about the quantity of previously sampled experi-  
 503 ments,  $n$ , to tune its hyperparameter. For example, as the  $n$  increases, LCB Adaptive decays its  $\beta$   
 504 hyperparameter value to become less explorative and more exploitative. Specifically, this informa-  
 505 tion feedback received by the function determines the contribution of both  $\mu(X)$  and  $\sigma(X)$  to the  
 506 acquisition value,  $a$ . Similar to EI Abrupt, LCB Adaptive computes an acquisition value,  $a \in [0, 1]$ ,  
 507 for a given  $X$ , wherein the  $X$  with the highest  $a$  is selected by the acquisition function as the next  
 508 suggested experiment to measure. LCB Adaptive is implemented for a minimization problem as:

$$a_{\text{LCB Adaptive}}(X, n; \beta, \epsilon) = \mu(X) - \epsilon^n \beta \sigma(X), \quad (4)$$

509 where  $n$  is the number of experiments sampled, and  $\beta = 3$  and  $\epsilon = 0.9$  are hand-tuned initialization  
 510 hyperparameters selected based on *a priori* domain knowledge of the function’s performance on a  
 511 variety of different problems. Having a large  $\beta$  and an  $\epsilon$  close to 1 supports a gradual decay from  
 512 very explorative to very exploitative, rather than a rapid decay. In the following section (Section A.2),  
 513 the dynamic EI Abrupt and LCB Adaptive are shown to both discover optima in fewer experiments  
 514 and avoid pigeonholing into local minima better than their static counterparts by actively balancing  
 515 the ratio of exploitation to exploration using learned information about the quality and quantity of  
 516 previously sampled experiments.

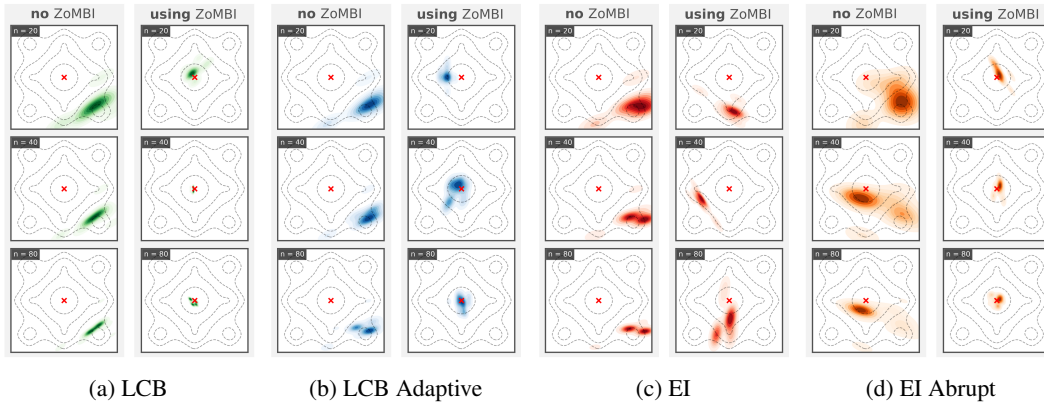


Figure A.1: **Acquisition Function Sampling Density.** The colored heatmaps indicate the regions of a 2D slice from a 5D Ackley function where sampling density is high for each respective acquisition function: (a) LCB, (b) LCB Adaptive, (c) EI, and (d) EI Abrupt. The contour lines indicate the manifold topology with local minima as the circular and pointed regions of the contours. The red "x" indicates the global minimum. For each acquisition function, the left panel shows the sampling density after  $n = \{20, 40, 80\}$  evaluated experiments without the use of ZoMBI while the right panel shows the sampling density after  $n = \{20, 40, 80\}$  evaluated experiments with the use of ZoMBI.

518 Pigeonholing into the local minima of a function occurs when an optimization algorithm has insuffi-  
 519 cient learned knowledge of the manifold topology to continue exploring potentially profitable regions  
 520 or when the algorithm's hyperparameters are improperly tuned, leading to overly exploitative tenden-  
 521 cies [1, 9]. The ZoMBI algorithm's anti-pigeonholing capabilities are two-fold: (1) the zooming search  
 522 bounds help the acquisition function to quickly stop sampling local minima once a better performing  
 523 data point is found and (2) actively learned acquisition function hyperparameters use knowledge about  
 524 the domain to help exit a local minimum. Figure A.1 demonstrates the anti-pigeonholing capabilities  
 525 of ZoMBI on optimizing a 5D Ackly function with both static and dynamic acquisition functions,  
 526 compared to that of traditional BO. The needle-like global minimum is indicated by the red "x" and  
 527 the local minima are indicated by the circular and pointed regions of the contour lines. The sampling  
 528 density of each acquisition function is illustrated by the heatmap, where the darker colors indicate  
 529 higher sampling density regions. The goal is to get high sampling density near the red "x". It  
 530 is shown that without ZoMBI being activated, the LCB, LCB Adaptive, and EI acquisition functions all  
 531 end up pigeonholing into local minima. However, EI Abrupt initially pigeonholes into a local minima  
 532 but then switches from an exploitative to an explorative mode to jump out of the local minimum  
 533 and converge closer to the global. Conversely, when running the optimization procedure with ZoMBI  
 534 active, all of the acquisition functions except the most exploitative, EI, converge onto the global  
 535 minimum fast. LCB Adaptive and EI are shown to initially start sampling towards a local minima,  
 536 but as ZoMBI is iteratively activated, the search bounds zoom in closer to the global minimum. Thus,  
 537 with the combination of active learning dynamic acquisition functions and zooming search bounds,  
 538 pigeonholing into sub-optimal local minima can be more readily avoided while optimizing Niah  
 539 problems, although avoidance is not guaranteed, as shown by the sampling density of EI.

### 540 **A.3 Rare Material Search Space Topology**

Table A.1: Description of variables from the two real-world Needle-in-a-Haystack materials science datasets [20].

Training Variable	Units	Description
Density	$\text{g/cm}^3$	Density of the entire molecule.
Formation Energy	$\text{eV/atom}$	Normalized change of energy to form target phase.
Energy Above Hull	$\text{eV/atom}$	Normalized energy to decompose into stable phase.
Fermi Energy	$\text{eV}$	Highest energy level at absolute zero.
Band Gap	$\text{eV}$	Valence to conduction band electron excitation energy

Target Variable	Units	Description
Poisson's Ratio, $\nu$	Unitless	Mechanical deformation perpendicular to the loading direction.
Thermoelectric Merit, $ZT$	Unitless	Electrical and thermal potential of a material to produce current.

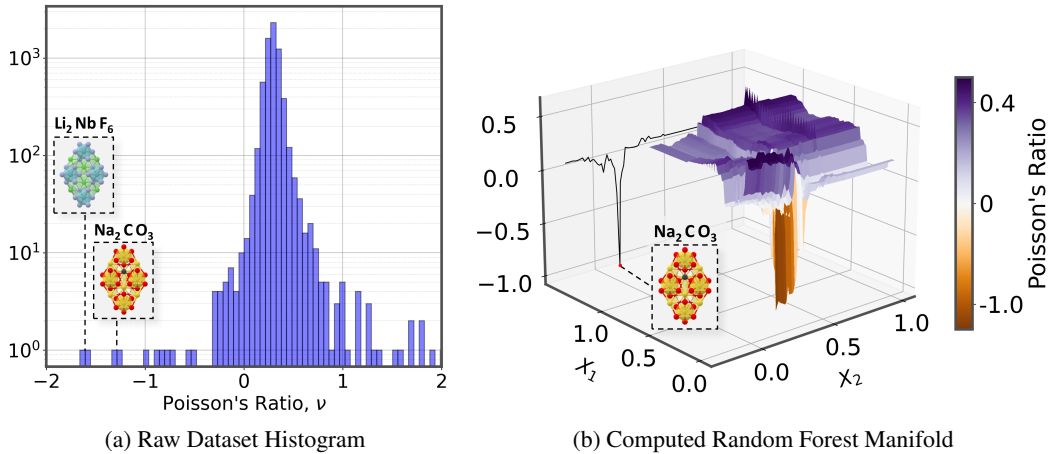


Figure A.2: **Histogram and Random Forest of Poisson's Ratio Dataset.** (a) The Poisson's ratio histogram of all 146k materials in the Materials Project Dataset [20, 21] with  $y$ -axis in log-scale. The two needles are called out, indicating the locations of minimum Poisson's ratio values  $\nu_{\min} = \{-1.2, -1.7\}$ . (b) The noisy, non-convex manifold topology generated by an RF regression of 500 trees on the Poisson's ratio dataset. A projected 2D slice of the 5D space is illustrate with  $z$ -axis and colorbar indicating the Poisson's ratio. The slice of space shown indicates the narrow basin of attraction region containing the  $\nu_{\min} = -1.2$  needle.

541 **A.4 ZoMBI Algorithm**

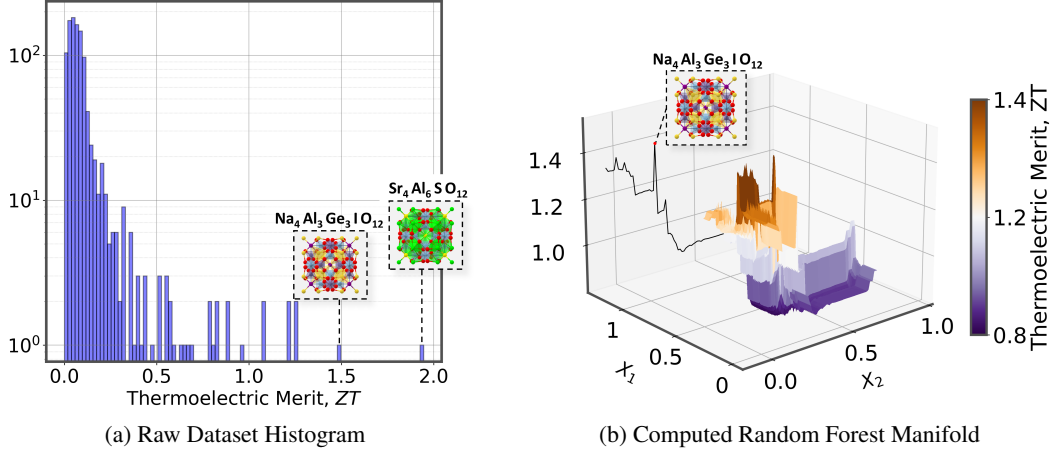


Figure A.3: **Histogram and Random Forest of Thermoelectric Merit Dataset.** (a) The Thermoelectric Merit,  $ZT$ , histogram of all 1k materials in the dataset computed by BoltzTraP [55, 20] with  $y$ -axis in log-scale. The two needles are called out, indicating the locations of maximum  $ZT$  values  $ZT_{\max} = \{1.4, 1.9\}$ . (b) The noisy, non-convex manifold topology generated by an RF regression of 500 trees on the  $ZT$  dataset. A projected 2D slice of the 5D space is illustrate with  $z$ -axis and colorbar indicating the  $ZT$  value. The slice of space shown indicates the narrow basin of attraction region containing the  $ZT_{\max} = 1.4$  needle.

---

**Algorithm 1:** Zooming Memory-Based Initialization (ZoMBI)

---

**Input :**  $\mathbf{X}$ : Set of data points  $\{X_1, X_2, \dots, X_n\}$ , where  $X_j \in \mathbb{R}^d$ ,  
 $\mathbf{y}$ : Set of target values  $\{y_1, y_2, \dots, y_n\}$ , where  $y_j \in \mathbb{R}$ ,  
 $\alpha$ : Number of ZoMBI activations,  
 $\phi$ : Number of forward experiments per activation,  
 $\gamma$ : Set of acquisition function hyperparameters  $\{\beta, \xi, \epsilon, \eta\}$ ,  
 $AF$ : An acquisition function selected by the user

**Output :** The next experimental condition  $X_{n+1} \in \mathbb{R}^d$  and measured target value  $y_{n+1} \in \mathbb{R}$

```

1 for  $\alpha$  activations do
2   Compute bounds  $\{\mathcal{B}_d^l, \mathcal{B}_d^u\} \leftarrow \{\min, \max\}_{X \in \mathbf{X}^{(m)}} \{[X]_d\}$ 
3   Initialize with  $i$  LHS data points  $\{X_i\} := \{X_1, X_2, \dots, X_i\}$ , where  $X_j \in \mathbb{R}^d, [\mathcal{B}_d^l, \mathcal{B}_d^u]$ 
   and target values  $\{y_i\} := \{y_1, y_2, \dots, y_i\}$ , where  $y_j \in \mathbb{R}$ 
4   Overwrite memory  $\mathbf{X} \leftarrow \{X_i\}$  and  $\mathbf{y} \leftarrow \{y_i\}$ 
5   for  $\phi$  forward experiments do
6     Let  $n = i + \phi$ 
7     Retrain surrogate model  $f(\mathbf{X})$  using target values  $\mathbf{y}$ 
8     Extract set of surrogate means  $\{\mu\}$  and variances  $\{\sigma\}$ 
9     Compute set of acquisition values  $\{a\} \leftarrow AF(\{\mu\}, \{\sigma\}; \gamma)$ 
10    Find the best new experimental condition  $X_{n+1} \leftarrow \arg \max \{a\}$ 
11    Measure target value of new experimental condition  $y_{n+1} \leftarrow f(X_{n+1})$ 
12    Append outputs to sets  $\mathbf{X}$ . append( $X_{n+1}$ ) and  $\mathbf{y}$ . append( $y_{n+1}$ )
13  end
14 end
```

---